atmosphere

Article

Robust Control of RSOC/Li-Ion Battery Hybrid System Based on Modeling and Active Disturbance Rejection Technology

Xiaolong Wu [1,2,3,*], Yu Li [1], Zilin Gao [1], Yuanwu Xu [4], Jingxuan Peng [3], Zhiping Xia [3], Lingyan Hu [1,5], Jiangong Hu [1,*], Zhuo Wang [3] and Xi Li [3]

1 School of Information Engineering, Nanchang University, Nanchang 330031, China
2 Shenzhen Research Institute, Huazhong University of Science and Technology, Shenzhen 518000, China
3 School of Artificial Intelligence and Automation, Huazhong University of Science and Technology, Wuhan 430074, China
4 School of Information Science and Engineering, Wuhan University of Science and Technology, Wuhan 430081, China
5 School of Electronic and Electrical Engineering, Shanghai University of Engineering Science, Shanghai 201620, China
* Correspondence: xiaolongwu@ncu.edu.cn (X.W.); jghu@ncu.edu.cn (J.H.)

Abstract: The application of new energy systems for industrial production to advance air pollution prevention and control has become an irreversible trend. This development includes hybrid systems consisting of reversible solid oxide cells (RSOC) and a Li-ion battery; however, at present the energy dispatching of such systems has an unstable factor in the form of poor heat/electricity/gas controllability. Therefore, the system studied in this paper uses the Li-ion battery as the energy supply/storage case, and uses the RSOC to supply power for the Li-ion battery charge or the Li-ion battery supply power to the RSOC for hydrogen production by water electrolysis. In this hybrid system, Li-ion battery thermoelectric safety and RSOC hydrogen production stability are extremely important. However, system operation involves the switching of multiple operating conditions, and the internal thermoelectric fluctuation mechanism is not yet clear. Therefore, in this paper we propose a separate control with a dual mode for hybrid systems. Active disturbance rejection control (ADRC) with a simple structure is used to achieve Li-ion battery module thermoelectric safety and control the hydrogen production/consumption of the RSOC module in the hybrid system. The results show that the required Li-ion battery thermoelectric safety and RSOC hydrogen consumption/production requirements can be met using the proposed controller, leading to a hybrid system with high stability control.

Keywords: solid oxide fuel cell (SOFC); Li-ion battery; active disturbance rejection control (ADRC); renewable energy system

check for updates

Citation: Wu, X.; Li, Y.; Gao, Z.; Xu, Y.; Peng, J.; Xia, Z.; Hu, L.; Hu, J.; Wang, Z.; Li, X. Robust Control of RSOC/Li-Ion Battery Hybrid System Based on Modeling and Active Disturbance Rejection Technology. *Atmosphere* **2023**, *14*, 947. https://doi.org/10.3390/atmos14060947

Academic Editor: Kumar Vikrant

Received: 8 April 2023
Revised: 30 April 2023
Accepted: 8 May 2023
Published: 29 May 2023

1. Introduction

In today's world, there is a growing demand for energy and fossil fuel resources. As conventional energy systems have caused environmental problems such as carbon emissions and the greenhouse effect, it is becoming necessary to develop new energy systems. Resource depletion and climate change are the main motivations for studying such systems [1,2]. In fact, RSOC/Li-ion battery hybrid systems composed of RSOC and Li-ion batteries can replace conventional power generation systems. As a clean energy source, the power generation/hydrogen production form of RSOC can help to accelerate carbon neutrality, while Li-ion batteries can compensate for the poor tracking characteristics of RSOC batteries [3–5]. Compared with other new energy systems, RSOC/Li-ion battery hybrid systems have advantages such as power generation/storage integration, high system efficiency, and suitability for islanded power generation and storage, and as such can reduce carbon dioxide (CO_2) emissions [6].

RSOC operation modes include solid oxide fuel cell (SOFC) mode and solid oxide electrolytic cell (SOEC) mode, which respectively provide the functions of power generation and hydrogen production and energy storage. As the ambient operating temperatures can be as high as 700–950 °C, if the high temperature waste heat generated by the RSOC is utilized, this can help to reduce carbon emissions and safeguard the atmospheric environment [6]. However, due to the high costs of RSOC development, most existing reversible fuel cell hybrid systems are based on proton exchange membrane-type fuel cells, which are more concerned with electrical management and water management issues. This is different from high-temperature hybrid systems in which SOFC is involved. However, hybrid systems constructed using a proton exchange membrane fuel cell and Li-ion battery can provide a reference for system integration. In this paper, system's waste heat is further exploited to enhance the system's temperature management [7]. The hybrid system integration proposed in this paper is novel, as the related research primarily addresses the stage of system integration in a single operating mode, which does not address the specific control issues of RSOC/Li-ion battery hybrid systems.

In an RSOC/Li-ion battery hybrid system, the Li-ion battery is mainly responsible for powering the external load, while the SOFC mode is mainly responsible for charging the Li-ion battery to replenish its consumed energy. The SOEC mode is mainly used to consume the electrical energy of the Li-ion battery to provide energy power for hydrogen production from electrolytic water. After the system is integrated, the management of thermoelectric characteristics is crucial. The Li-ion battery constantly changes its power and discharges irregularly due to the changing demand of external loads. At this point, higher demands are placed on the power replenishment of the SOFC subsystem and the SOEC electrolysis for hydrogen production. However, to the best of our knowledge there are few works related to this topic. In contrast, scholars have conducted preliminary works on thermoelectric power management in stand-alone SOFC or Li-ion battery energy storage systems. For example, Cen et al. used a basic finned-tube heat exchanger structure and a special aluminum frame to design a cylindrical Li-ion-ion battery pack thermal management module for use at extreme ambient temperatures. The temperature of the battery pack can be easily controlled to a preset value of 40 °C [8]. Cui et al. proposed a robust predictive energy management strategy based on a thermoelectric cooler. This strategy can regulate the battery temperature within the appropriate range and reduce energy consumption, guaranteeing the thermal safety of the Li-ion battery while satisfying the electrical load [9]. Wu et al. developed four nonlinear model predictive controllers based on back-propagation (BP) neural networks. Such controllers can track the load and maintain the proper temperature under fuel leak failure, air compressor failure, and SOFC normal conditions [10]. From the above works, it is easy to see that the thermoelectric fluctuation problem is a common problem in hybrid systems; however, the existing solutions are mostly based on predictive control approaches. This is not conducive to the implementation of control schemes. Because predictive control often requires high model accuracy, even a slight deviation of the model usually results in unpredictable control consequences [11–13].

In order to ensure the operability of the control scheme at a later stage, researchers have proposed an ADRC method for hybrid Li-ion battery and fuel cell systems [14–17]. This method is an evolution of traditional PID control [18–20], which does not require high model accuracy and is widely used in industrial power applications. For example, Wu et al. studied the control problem of grid-connected SOFC power plants under load variation and uncertainty in network parameters. They used ADRC to improve the performance of a power regulation system consisting of a DC–DC converter and a DC–AC inverter. Their results showed that ADRC has more stable performance than conventional proportional–integral (PI) controllers for grid current control [21]. Curiel-Olivares et al. oriented a two-wheeled self-balancing electric vehicle powered by a Li-ion battery. They proposed a robust self-balancing control scheme based on ADRC, and the results showed that the Li-ion battery exhibited robustness in power supply [22]. This provides an excellent reference for the research in this paper.

In the present paper, a study of the thermoelectric control of an RSOC/Li-ion battery hybrid system is carried out by constructing a mechanism model. The paper addresses the design of robust controllers using a simple, general, and practical control method, namely, the ADRC method [23–25]. Two control problems in hybrid power generation systems are discussed: (i) regulation of the Li-ion battery charging and discharging temperatures along with voltage fluctuations; and (ii) control of thermoelectric performance and hydrogen production in a dual-mode (SOFC and SOEC modes) hybrid system. Although there is little previous research available in the literature on the control of RSOC/Li-ion battery hybrid systems, we hypothesize that this approach can be applied to the control of hybrid RSOC/Li-ion battery systems by learning from existing control methods for hybrid systems in related fields [26–29]. Therefore, the main contribution of this paper is the introduction of a simple and practical controller for RSOC/Li-ion battery hybrid systems. This controller is able to perform the tasks of ensuring thermoelectric safety and load tracking despite external excitation and disturbance and/or self-perturbations. In addition, the model proposed in this paper achieves good closed-loop performance under conditions of various uncertainties and external perturbations.

The rest of this work is organized as follows. In Section 2, the mechanistic equation model of the baseline the RSOC/Li-ion battery hybrid system is described, as well as the main ideas involved in the design of a robust controller. Section 3 presents the closed-loop performance of the proposed controller for two control tasks: (i) the regulation of Li-ion battery charging/discharging temperatures and voltage fluctuations; and (ii) control of thermoelectric performance and hydrogen production in a dual-mode (SOFC and SOEC) hybrid system. In Section 4, we present a discussion of our results and their practical implications. Finally, in Section 5, we provide our conclusions and remarks on future research prospects.

2. Materials and Methods

The system mechanism model for the RSOC and Li-ion battery integration is introduced first in this part. Then, based on the concept of ADRC, the general method used for controller development is presented.

2.1. Dynamic Power Generation Process of RSOC/Li-Ion Battery Hybrid System

An RSOC/Li-ion battery hybrid system is composed of hydrogen, air, external load current, a hydrogen storage tank, a Li-ion battery, and other components. The schematic diagram of such a hybrid system is shown in Figure 1. The power generation process is as follows [30,31].

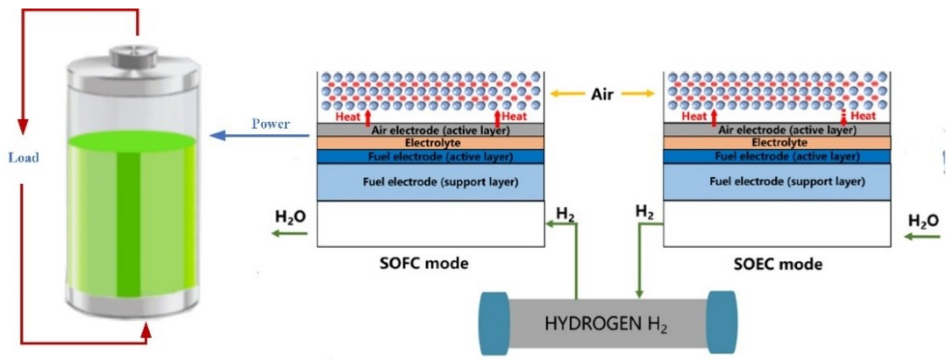

Figure 1. Diagram of hybrid system.

(1) When the SOFC mode is not operating, H_2O and load are introduced into the system, then the Li-ion battery starts to generate electricity for the load. The RSOC is in SOEC mode and the system starts to produce hydrogen by water electrolysis, which is stored in the hydrogen storage tank. The SOEC working mode requires an external power supply, and achieves the purpose of hydrogen production by water electrolysis.

(2) When the Li-ion battery experiences discharge over a long time, its remaining power is insufficient. In this state, the SOFC mode begins working and the hydrogen tank starts to supply hydrogen to ensure that the RSOC module can generate electricity for the Li-ion battery, providing the Li-ion battery with a power boost. When the Li-ion battery is fully charged, the SOFC mode is deactivated and the SOEC mode works to replenish the hydrogen consumed in the hydrogen storage tank.

Normal operation of the above process can effectively maintain mutual transfer of energy and material change between the RSOC and the Li-ion battery in an integrated hybrid system.

Following the pioneering study of Zhang et al., several authors have considered the problem of slow SOFC load tracking [32]. Cheng et al. considered the inclusion of an observer in the control process to ensure thermal safety inside the stack [33]. Previous works have pointed out a number of characteristics of SOFC systems: (i) the SOFC has strong thermoelectric coupling characteristics, and the thermal and electrical response rates are on the order of seconds and milliseconds, respectively; (ii) temperature safety can be accomplished by reducing the load current; and (iii) the thermal gradient of the SOFC often needs to be controlled within 100 °C.

In fact, when the hybrid system starts to generate electricity, the thermal safety of the Li-ion battery needs to be considered as well, as the whole process is an exothermic reaction. In addition, the choice of control method affects both the thermoelectric control and hydrogen production effect of the hybrid system.

The operational issues mentioned above have motivated different works to improve the technical and operational performance of solid oxide and Li-ion batteries. These works include analysis of thermoelectric performance and data preprocessing for both types of battery mentioned above [34,35], integration of Li-ion battery charging and discharging technology, electrolytic water hydrogen production technology with RSOC/Li-ion battery hybrid systems [36,37], improvement of control strategies using mechanistic modeling, and development and application of different control designs.

2.2. RSOC/Li-Ion Battery Hybrid System Model

Simulink models were connected based on the architecture of the hybrid system according to the physical first principles (conservation of mass, conservation of energy, conservation of matter, etcetera). Among them, the RSOC module and the Li-ion battery module are constructed using basic mechanistic equations such as the Nernst equation, heat exchange, and electrochemical reflection combined with available heat–electricity–gas measurements for modeling and analysis. Zhang et al. [38] set up three hybrid system operation scenarios to derive their RSOC/Li-ion battery hybrid system model. The proposed model was developed for the control needs of RSOC/Li-ion battery hybrid systems. The experimental arrangement and conditions were characterized and described by Zhang et al. [39].

The specific modeling process is described in the following two subsections.

2.2.1. RSOC System Module

To accommodate the Li-ion battery module data, the model for the RSOC module makes the following assumptions [40]:

(1) A constant gradient of air pressure drop in the direction of the air flow;
(2) The system components are adiabatic from the outside;
(3) The edge effects of the RSOC stack are neglected, and all single cells (consisting of PENs and adjacent metal linkers) have exactly the same dynamic behavior;
(4) The metallic linker has good electrical conductivity, with equal potential at all points;
(5) All heat generated by the electrochemical reaction is released in the PEN of the single cell;
(6) Adiabasis exists between adjacent single-cell bodies;
(7) The RSOC has 100% current efficiency, i.e., the number of electrons produced by the hydrogen electrochemical reaction is theoretical;

(8) In each gas supply subsystem, the hysteresis characteristics of the airflow caused by the gas supply piping and mass flow meter can be replaced by an inertial link and delayed link equivalent.

The generic part of the specific modeling equations is shown in Table 1 below.

Table 1. Modeling mechanism equations for RSOC modules and auxiliary components.

Model Name	Mechanism Equation
Flow rate model	$\dot{N}_{out} = \dot{N}_{in} + \sum R_i, i \in \{H_2, O_2, H_2O, N_2\}$
Molar fraction model	$N\frac{dX_i}{dt} = \dot{N}_{in}X_{i,in} - \dot{N}_{out}X_{i,out} + R_i, i \in \{H_2, O_2, H_2O, N_2\}$
Temperature model	$NC_V\frac{dT}{dt} = \dot{N}_{in}h_{in} - \dot{N}_{out}h_{out} + \sum \dot{Q}_{in}$
Fluid molar enthalpy	$h_i = h_{i,298.15} + \int_{298.15}^{T} C_{P,i}(T)dT, i \in \{H_2, O_2, H_2O, N_2\}$
Solid unit temperature model	$\rho_s V_s C_s \frac{dT}{dt} = \sum \dot{Q}_{in}$
RSOC thermal model	$\rho_{PEN} V_{PEN} C_{PEN} \frac{dT_{PEN}}{dt} = \sum \dot{Q}_{in,PEN} + \dot{Q}_{react} - \dot{W}_{out}$
Air supply module time-delay model	$G(s) = \frac{1}{Ts+1}e^{-\tau s}$
Nernst equation model	$E = E^0 \pm \frac{RT}{nF}\ln\frac{C^c D^d}{A^a B^b}$

Additional mechanistic equations and related explanations of the relevant variables can be found in the literature [40]. These parameters were obtained using parameter identification methods developed in the course of previous work by our research group [40].

2.2.2. Li-Ion Battery Module Model Description

(1) Temperature model of Li-ion battery [41]:

$$\begin{aligned} dTc &= \frac{1}{Cc}(Q + (Ts - Tc)/Rc)dt \\ dTs &= \frac{1}{Cs}((-Ts + Tc + (Tf - Ts)/Ru)/Rc)dt \end{aligned} \tag{1}$$

where Ts and Tc are the surface temperature and internal core temperature of the Li-ion battery, respectively, while Cs and Cc are the coefficients of the surface and internal core of Li-ion battery, respectively. The set values were Cs = 4.5, Cc = 62.7; Ru = 15, and Rc = 1.94; these parameters are set based on empirical judge.

(2) Electrochemical model of Li-ion battery [42]

Assuming that the performance of the active substance inside the electrode changes only in the x-axis direction, the specific relationship is as follows:

$$\eta = \phi_s - \phi_e - U_{ocp} - jFR_{film} \tag{2}$$

where ϕ_s and ϕ_e are the solid phase electrode and electrolyte potential, respectively, U_{ocp} is the open circuit voltage, and R_{film} is the diaphragm resistance. From the Butler–Volmer equation, the cell current density is obtained as follows:

$$j(x,t) = kc_e^{1-\alpha}(c_{max} - c_{s,e})^{1-\alpha}c_{s,e}^{\alpha}\left\{\exp\left[\frac{(1-\alpha)F}{RT}\eta\right] - \exp\left(-\frac{\alpha F}{RT}\eta\right)\right\} \tag{3}$$

The relationship between the concentration of the solid-phase electrode and the potential is expressed as

$$\begin{aligned} &\frac{\partial c_s(r,x,t)}{\partial t} = \frac{D_s}{r^2}\frac{\partial}{\partial r}\left[r^2\frac{\partial c_s(r,x,t)}{\partial r}\right] \\ &\frac{\partial}{\partial x}\left[\sigma^{\mathrm{eff}}\frac{\partial}{\partial x}\phi_s(x,t)\right] - a_s F j(x,t) = 0 \end{aligned} \tag{4}$$

The relationship between the concentration of the liquid-phase electrolyte and the potential is expressed as

$$\begin{aligned} &\frac{\partial[\varepsilon_{\mathrm{e}} c_{\mathrm{e}}(x,t)]}{\partial t} = \frac{\partial}{\partial x}\left[D_{\mathrm{e}}^{\mathrm{eff}}\frac{\partial}{\partial x}c_{\mathrm{e}}(x,t)\right] + \left(1 - t_+^0\right)a_s j(x,t) \\ &\frac{\partial}{\partial x}\left[k^{\mathrm{eff}}\frac{\partial}{\partial x}\phi_{\mathrm{e}}(x,t)\right] + \frac{\partial}{\partial x}\left[k_D^{\mathrm{eff}}\frac{\partial}{\partial x}\ln c_{\mathrm{e}}(x,t)\right] + a_s F j(x,t) = 0 \end{aligned} \tag{5}$$

The microscopic particle variation of the Li-ion battery is shown in the above equation, which is known as a pseudo-2D model. Based on this model, the performance of the battery can be estimated after mathematical derivation.

(3) Feature Parameter Selection

For control design purposes, the state vector is shown as $x = [x1, x2, x3, x4, x5, x6, x7, x8, x9, x10, x11, x12]^T = [\dot{N}_{H_2}, \dot{N}_{H_2O}, \dot{N}_{air}, P, I, R_{film}, p_{H_2}, p_{H_2O}, T_{c,Li\text{-}ion}, T_{s,Li\text{-}ion}, T_{RSOC}, U_{ocp}]^T$. Here, $\dot{N}$ is the flow rate, P is the power in charging or discharging condition, T is the temperature, I is the current, p is the pressure, R is resistance value, and U is voltage. Nominal operation was simulated using the parameter values shown in Table 2 below [40].

Table 2. Key parameters of the RSOC module.

Parameter Name	Parameter Value
Anode convection coefficient (kW/m^2 K)	0.05
Cathode convection coefficient (kW/m^2 K)	0.05^2
PEN conduction coefficient (kW/m K)	2×10^{-3}
IC conduction coefficient (kW/m K)	25×10^{-3}
PEN density (kg/m^3)	5900
IC density (kg/m^3)	9000
PEN specific heat capacity (kJ/(kg K))	0.5
IC specific heat capacity (kJ/(kg K))	0.62
The porosity	0.4
Pore size (up)	0.5
The activation energy of anode (J/mol)	1×10^5
The activation energy of cathode (J/mol)	1.2×10^5
Limitation current density (A/m^2)	10,000
The node of a single cell	5
The number of cells in stack	13
The width of a single cell (m)	0.10
The length of a single cell (m)	0.10

Table 2. *Cont.*

Parameter Name	Parameter Value
The area percent of gas though the cell	0.95
The thickness of PEN (m)	0.5×10^{-3}
The thickness of IC (m)	1×10^{-3}
The highness of anode channel (m)	1×10^{-3}
The highness of cathode channel (m)	2×10^{-3}
The pressure difference in anode channel (pa)	0.05×10^{5}
The pressure difference in cathode channel (pa)	0.05×10^{5}

Figure 2 shows the temperature variation of the Li-ion battery in charging and discharging modes. The Li-ion battery indicators display voltage fluctuations in both discharging (Time is 20 s in Figure 2a) and charging (Time is 40 s in Figure 2b) modes. However, the Li-ion battery temperature rises at a fast rate, which is detrimental to the Li-ion battery's thermoelectric safety. On the other hand, the hidden danger of Li-ion battery thermoelectric safety is transferred to the RSOC module in the hybrid system, which affects the performance of the RSOC stack and its auxiliary components.

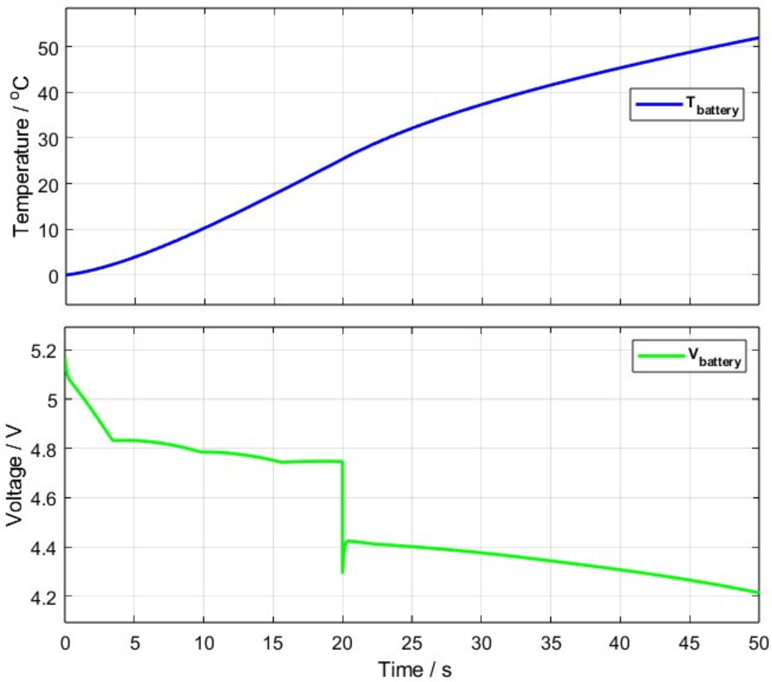

(**a**) Discharge situation

Figure 2. *Cont.*

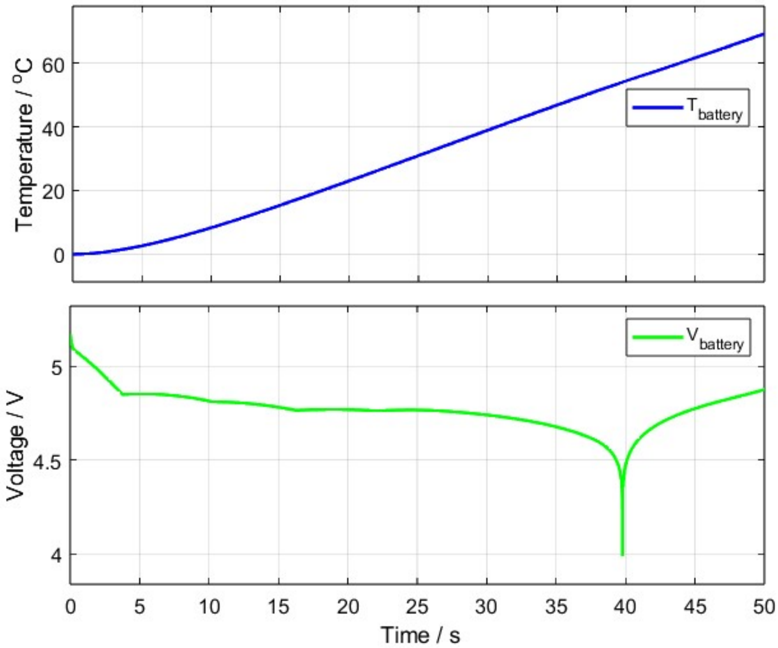

(**b**) Charging situation

Figure 2. Temperature and voltage variation of Li-ion battery in charging and discharging modes.

2.3. Control Design Method Based on ADRC

In order to avoid the situation described in Figure 2, this research uses the ADRC control method, which has significant advantages for handling fluctuation problems. The ADRC algorithm incorporates PID control ideas and modern control theory. This algorithm can select the integral standard type according to the input and output of the complex controlled system, which can eliminate the external unknown disturbance and compensate for the internal uncertainty of the system while allowing for real-time estimation and compensation of the disturbance [43–45]. The ADRC method is based on a model-free approach for simple controller development. However, as RSOC systems are less popular in physical form, in this paper we mainly use models to replace the concept of physical prototypes. Therefore, the controller design in this paper is established based on the system models constructed in Section 2.2. Because these models contain elements driven by the presence of data, they are uncertain with envelope constraints, and the observer embedded in the ADRC controller has the function of monitoring the system state variables. The state variables are monitored by the observer, which in turn enables the compensation output of the controller. The ADRC method was first proposed by Han et al. [46]. Tan et al. [47] extended the initial idea to power systems and studied linear active disturbance suppression control. Li et al. [48] proposed an ADRC with a switching law to address the problem of accurate temperature regulation in PEMFC. The ADRC method has been widely used, and is considered an effective technique for dealing with uncertain nonlinear systems in complex chemical and energy field processes [47–49].

Aiming at the RSOC/Li-ion battery hybrid system with nonlinear and uncertain characteristics of the mechanism model in the power generation process, this paper introduces the ADRC technique to the RSOC/Li-ion battery hybrid system. This controller consists of Tracking Differentiator (TD), Non-Linear States Error Feedback (NLSEF), and Extended States Observer (ESO) links. In designing the ADRC controller, v is the input of the system, v_1 is the tracking value of v, v_2 is the differential value of v_1, e_1 and e_2 represent the error, z_1, z_2, and z_3 are the perturbation estimates, $e_1 = v_1 - z_1$, $e_2 = v_2 - z_2$, b is the compensation factor, u_0 is the control law, u is the actual control amount, β_1 and β_2 are the gain parameters, and y is the output of the system. The ADRC control structure is illustrated in Figure 3. The role of the radial basis function neural network (RBFNN) is to tune the parameters of the ADRC controller.

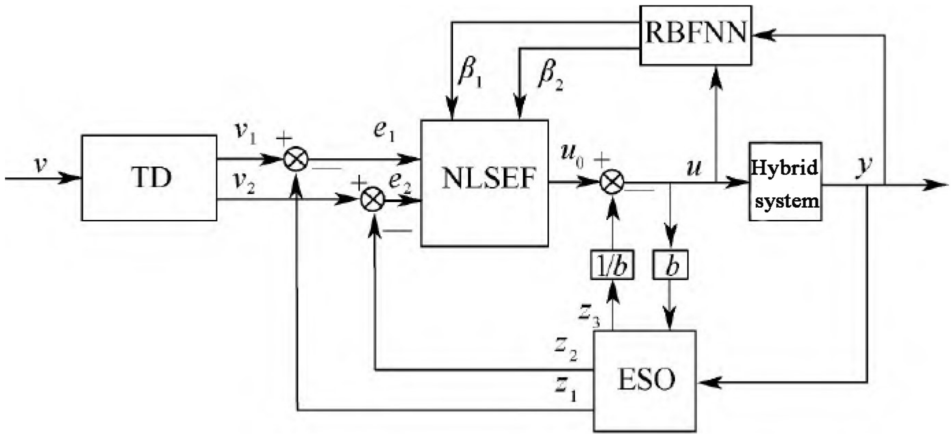

Figure 3. Structure diagram depicting active disturbance rejection control for an RSOC/Li-ion battery hybrid system.

To prevent the input signal from directly affecting the controlled object and causing the output signal to overshoot, a transition process TD module is designed that can quickly track the input signal and extract the differential signal of the tracked signal. The fast optimal synthesis function $fal(.)$ algorithm is introduced to design the discrete tracking differential signal as follows [46]:

$$\begin{cases} v(k+1) = v_1(k) + hv_2(k) \\ v_2(k+1) = v_2(k) + h\varphi \\ \varphi = \text{fhan}(v_1(k) - v(k), v_2(k), r, h_0) \end{cases} \tag{6}$$

where r is the fast factor, h is the sampling period, and h_0 is the filtering factor. The ESO considers the system from the perspective of unmodeled dynamics, uncertain parameters, and unknown external disturbances, then observes and compensates for the system state in real time using the output feedback design, resulting in a system without static error control. ESO does not require an accurate and rigorous mathematical model of the controlled object, meaning that disturbance observation can be achieved without direct measurements. The hybrid system disturbance is set to the expansion state x_3, and the unknown variable x_3 is estimated such that the value of z_3 is obtained as follows [46]:

$$\begin{cases} e = z_1 - y \\ \dot{z}_1 = z_2 - \mu_1 e \\ \dot{z}_2 = z_3 - \mu_2 fal(e, \alpha_1, \delta) + bu \\ \dot{z}_3 = \mu_3 fal(e, \alpha_2, \delta) \end{cases} \tag{7}$$

where μ_1, μ_2, and μ_3 are adjustable gain parameters, α_1 and α_2 are design parameters, δ is the width of the nonlinear interval, and $fal(e, \alpha_2, \delta)$ is the nonlinear saturation function, denoted as

$$fal(e, \alpha_1, \delta) = \begin{cases} |e|^{\alpha}\text{sgn}(e), |e| > \delta \\ \dfrac{e}{\delta^{1-\alpha}}, |e| \leq \delta \end{cases} \tag{8}$$

The discrete equation of state for the observer is as follows:

$$\begin{cases} e = z_1(k) - y(k) \\ z_1(k+1) = z_1(k) + hz_2(k) - h\mu_1 e \\ z_2(k+1) = z_2(k) + h(z_3(k) - \mu_2 fal(e, \alpha_1, \delta) + bu) \\ z_3(k+1) = z_3(k) - h\mu_3 fal(e, \alpha_2, \delta) \end{cases} \tag{9}$$

NLSEF uses the $fal(\cdot)$ "large error with small gain" and "small error with large gain"; essentially, the control law u_0 is obtained according to the error signal e, then the actual control amount is obtained by compensating for the estimated value of disturbance z_3. The NLSEF is designed as follows:

$$u_0 = \beta_1 fal(e_1, \alpha_3, \delta) + \beta_2 fal(e_2, \alpha_4, \delta) \tag{10}$$

where α_3 and α_4 are the design parameters.

In summary, the actual amount of control available for the hybrid system is $u = u_0 - z_3/b$.

In this paper, the ADRC method is applied to the RSOC/Li-ion battery hybrid system model under the following additional assumptions.

Assumption 1: The temperature and voltage of the Li-ion battery are the key control variables, i.e., $u = [T_{Li-ion}, V]$. Assumption 2: The control input is affected by the saturation nonlinearity, i.e., $u_{min} \leqslant u \leqslant u_{max}$. Assumption 3: The controlled variables can be used for control design purposes. The following comments are necessary at this point:

A. For control purposes of the hybrid system power generation or hydrogen production process, in practice only a relatively limited amount of control is usually possible. Most of these actions are limited to the Li-ion battery thermoelectric safety state and the operating conditions of the RSOC module. Therefore, in this paper the hydrogen consumption, hydrogen production, RSOC module voltage, Li-ion battery voltage, and surface temperature are selected as the key indicators for reference.

B. According to previous works on the operation process of the hybrid system model, the Li-ion battery temperature control is very important and must be attended to in order to ensure safe and long-lasting operation of the Li-ion battery module.

3. Results

In this section, two control problems are addressed in the mechanism equation model constructed based on the above ADRC control method: (i) regulation of the Li-ion battery charging/discharging temperatures and voltage fluctuation; and (ii) control of the thermoelectric performance and hydrogen production in dual-mode operation (SOFC and SOEC modes) of the hybrid system. The control effect of the ADRC controller is tested, and the fast and stable operation processes of the hybrid system are respectively studied in dual-mode operation.

In order to fully investigate the hybrid system's steady-state operation conditions, two control variables are selected as benchmarks in this paper to facilitate the evaluation of control effects and enable rational decision-making. We first select the range of Li-ion battery module current variation and the range of RSOC module current variation during the operation of the hybrid system; the fluctuation range is shown in Figure 4. It should be noted that during the transition from charging to discharging the current undergoes an approximate step transition between 100 s and 150 s. In the Li-ion battery charging phase (time after 150 s), the current value is stable at about 80 A, while in the discharging phase the Li-ion battery module current is about −80 A. Therefore, in this paper we conduct a control analysis of the thermal–electrical–pneumatic characteristics of the hybrid system within the current regulation interval of the Li-ion battery module.

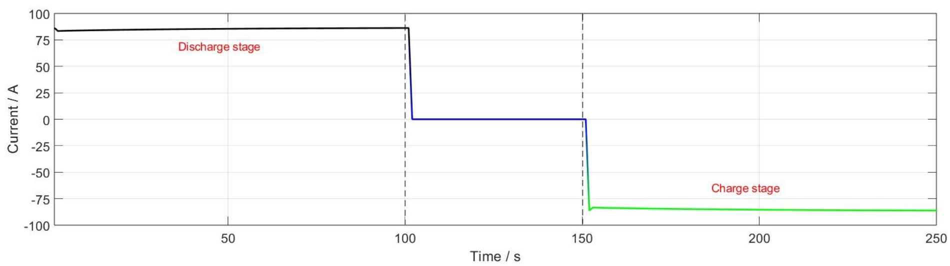

Figure 4. Current trend setting for Li-ion battery modules in the control process.

3.1. Control of Li-Ion Battery Thermoelectric Characteristics in Dual-Mode Operation

3.1.1. Control Problem

First, the RSOC module voltage value and the Li-ion battery thermostat value are set. The control problem is set to regulate the voltage and temperature values of the Li-ion battery to the desired reference values, thereby achieving efficient control. The Li-ion module temperature is related to the RSOC module discharge current and the surface temperature of the Li-ion module. Therefore, the main adjustment variable in the regulation process is the voltage value of the RSOC module in SOFC mode. At the same time, the surface temperature of the Li-ion battery module is controlled as much as possible, satisfying the thermoelectric safety requirement of the Li-ion battery module in the charging phase. When performing control, the hydrogen supply is considered to have a constant value $N_{h2} = 0.006$ mol/s.

3.1.2. Numerical Results

The first step in designing the ADRC controller is to construct an input–output mechanism model that can reflect the relationship between the external input voltage of the RSOC module or demand for hydrogen production on the one hand, and the Li-ion battery module on the other. This is the model described in Section 2. The model follows a second-order approach when using ADRC to control the temperature of the Li-ion battery, and the control parameters are b0 = 0.01, wc = 1, and wb = 15. ADRC controls the voltage input of the RSOC module, with the parameters set as follows: b0 = 0.06, wc = 0.02, and wb = 0.08. The PID controller controls the temperature of the Li-ion battery, and the parameters are set to P = 0.7, I = 1, D = 0, filter coefficient N = 10, Wb = 1, and Wc = 1. Optimisation of the ADRC controller parameters is done by RBFNN from Figure 3. The PID controller controls the voltage input of the RSOC module, with the parameters set as P = 1, I = 1, D = 0, filter coefficient N = 100, Wb = 1, and Wc = 1.

Figure 5 shows the output response characteristics of the hybrid system after adjusting the parameters of the ADRC controller and the PID controller. Under the hybrid model, the control effect is tested using the PID controller and ADRC controller, which are then compared.

From Figure 5, the ADRC controller can adjust the Li-ion battery temperature and voltage to the expected values while minimizing the impact of external disturbances. The expected value of the control input is set as follows: temperature = 25 °C and voltage value = 4.5 V. The observed control results are as follows.

(1) When the hybrid system is running in SOFC mode, the voltage value of the Li-ion battery is stable at 4.6 V after the ADRC controller runs for 5 s. The surface temperature of the Li-ion battery can be stabilized at 25 °C after 8 s. Under the action of the PID controller, after the system runs for about 70 s the surface temperature of the Li-ion battery is 25 °C. The Li-ion battery voltage shows a slow upward trend after 9 s, and reaches 4.9 V in 100 s. It can be seen that the performance of the ADRC controller is significantly better than that of the PID controller when operating in SOFC mode, mainly in terms of rapid temperature control and voltage stability (Figure 5a).

(2) When the hybrid system is running in SOEC mode, the Li-ion battery is in its discharge phase. It can be seen from Figure 5 that the voltage of the Li-ion battery has a downward trend. Under the action of the ADRC controller, the temperature of the Li-ion battery first decreases and then increases in the first 5 s, followed by a returned to the stable state at 25 °C. In the first 75 s, the voltage value of the Li-ion battery is in a state of slow decline, while after 75 s the voltage of the Li-ion battery is stable at 1.3 V. In addition, under the action of the PID controller it is obvious from Figure 5b that the temperature of the Li-ion battery is difficult to control within 100 s at 25 °C. However, the change trend of the voltage value is essentially consistent with the action of the ADRC controller.

It can be seen that the performance of the ADRC controller is significantly better than that of the PID controller in dual-mode, which is mainly reflected in the rapid control of the temperature and the stability of the voltage value.

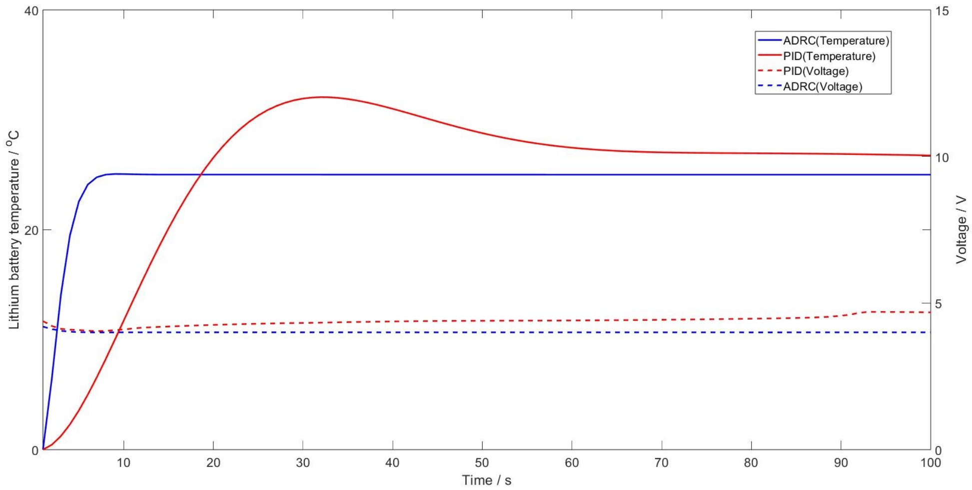

(**a**)

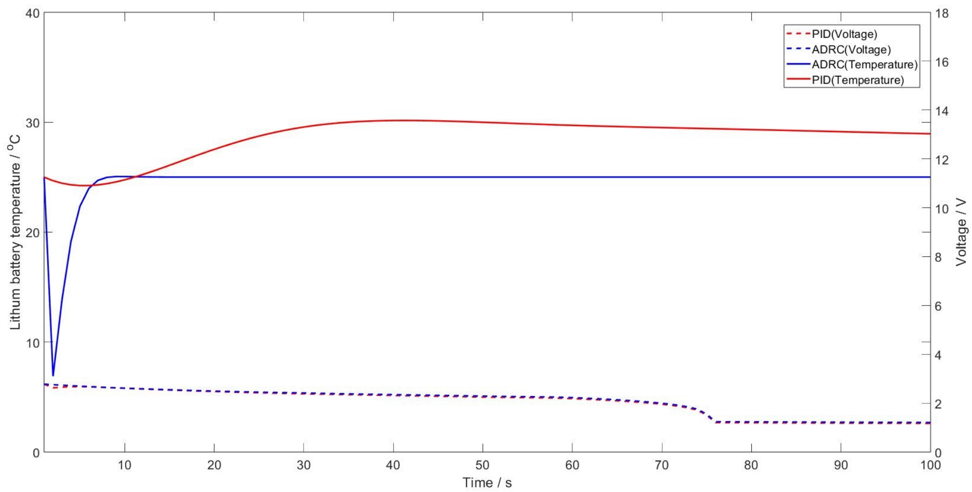

(**b**)

Figure 5. The temperature and voltage response curves of the Li-ion battery module in the hybrid system in hydrogen production mode and Li-ion battery charging mode. (**a**) Response curves of the Li-ion battery temperature and voltage under PID and ADRC controllers in SOFC mode (Li-ion battery charging) and (**b**) response curves of the Li-ion battery temperature and voltage under PID and ADRC controllers in SOEC mode (Li-ion battery discharge hydrogen production).

3.2. Hydrogen Consumption and Hydrogen Production Control in Dual Mode

3.2.1. Control Problem

During operation of the hybrid system, hydrogen production by water electrolysis and hydrogen consumption for power generation are very important. When electrolyzing water to produce hydrogen, it is necessary to properly control the power supply of the external Li-ion battery such that hydrogen can be produced stably in SOEC mode. In addition, in power generation mode the stability of hydrogen consumption is key to ensuring the stable operation of the system. Therefore, hydrogen control with respect to hydrogen production and the hydrogen production process is particularly important.

3.2.2. Numerical Results

For this control problem, we use two control methods in this section for testing, namnely, PID and ADRC. We set the RSOC module voltage input to a constant value of 0.56 V, and the two specific types of situations are as follows:

(1) In SOFC mode, the parameters of the PID controller are set as follows: P = 0.03, I = 0.0002, D = 0.002, filter coefficient N = 1000, Wb = 0.2, and Wc = 0.08, while the surface

temperature of the Li-ion battery is 25 °C and the voltage of the Li-ion battery is 2.6 V. The corresponding hydrogen consumption is shown in Figure 6a. When using the ADRC control method, the parameters of the ADRC controller are set as follows: b0 = 1, Wc = 0.02, and Wb = 0.08; the hydrogen consumption trend is shown in Figure 6a. It can be seen from Figure 6 that the hydrogen consumption controlled by ADRC is relatively stable and the molar flow rate is low, which can effectively ensure the high power generation efficiency of the hybrid system.

(2) In SOEC mode, the parameters of the PID controller and ADRC controller are set according to the hydrogen production demand of 0.047 mol/s; the parameter table is shown in Table 3.

Table 3. Control parameters.

Parameter No.	ADRC		PID	
1	W_b	0.04	W_b	1
2	W_c	0.06	W_c	1
3	b_0	0.005	Filter coefficient	100
4	Order	2	P	0.5
5	Time domain	continuous	I	1
6	–	–	D	1

When operating in SOEC mode, the control problem should be the same as that of thermoelectric control problem for the Li-ion battery module. Two types of controllers are used to adjust the hydrogen production to the required reference value while rejecting external disturbances.

When the hybrid system is running in SOEC mode, the Li-ion battery is in a discharged state. It can be seen from Figure 6b that, under the action of the ADRC controller, the hydrogen production of the system shows an upward trend (overshooting) in the first 10 s; the hydrogen production of the hybrid system then gradually decreases after 10 s and stabilizes at 0.047 mol/s by 33 s. The main difference is that the control effect of PID controller is slightly worse than that of ADRC controller. Specifically, the preset hydrogen production cannot be tracked accurately, and its deviation from the ideal value is greater than the deviation between the ADRC controller and the ideal value.

It can be seen that the ADRC controller performs well in terms of both hydrogen production and hydrogen consumption when operating in dual mode. At the same time, the hydrogen consumption/hydrogen production effect obtained by the ADRC controller is significantly better than that of the PID controller.

Regarding the comparison between the proposed controller and the classical PID controller, the following observations can be made with respect to the two control problems. (i) When the controller is involved, the control effect is significant (compare Figures 2 and 6). At the same time, the output effect obtained by the control input through the ADRC controller is better than that of the PID controller. In this way, the hydrogen production capacity, the temperature of key positions in the RSOC system, and the power generation control of the hybrid system are all faster, more stable, and more accurate. (ii) The control effect of ADRC controller is satisfactory. Although there is an overshoot in the hydrogen production control process, this does not affect the storage of hydrogen. At the same time, the system has a good control effect on temperature and voltage in SOFC/SOEC dual-mode operation, and no overshooting occurs.

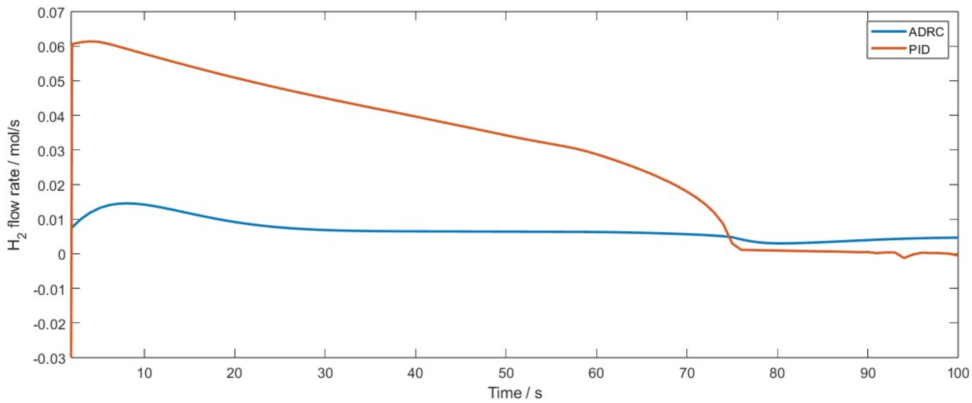

(**a**) Hydrogen consumption in SOFC mode

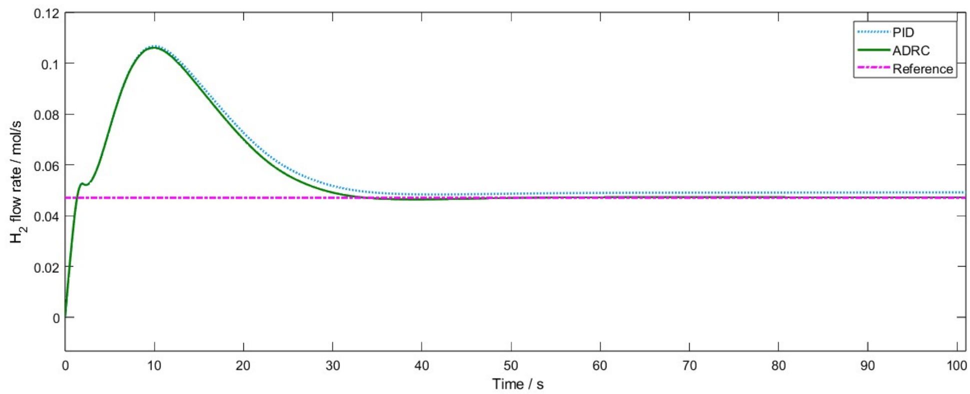

(**b**) Hydrogen production in SOEC mode

Figure 6. Hydrogen flow rates for the hydrogen consumption and hydrogen production processes during SOFC/SOEC dual-mode operation.

4. Discussion

The following discussion is based on the numerical simulation of the proposed control scheme.

With regard to the temperature value and voltage value of the Li-ion battery module, the Li-ion battery module's operation is significantly affected by the thermoelectric performance of the RSOC module [39]. This paper draws on the thermal analysis method of Li-ion batteries by Chen et al. [50], on the basis of which we have conducted in-depth research on selected parameter values such as the hydrogen production/hydrogen consumption, battery surface temperature, and hybrid system power generation. The key to controlling the hybrid system was found to be the management of the thermoelectric parameters for the Li-ion battery module. The Li-ion battery module uses the power generated by the RSOC module for charging, which affects its own temperature. Under the action of the controller, the thermal safety of the Li-ion battery can be guaranteed and the Li-ion battery module can be charged smoothly. Xue et al. [51] have argued that when external perturbations are applied the temperature value for the RSOC module must not be higher than 900 °C during the operation of the RSOC/Li-ion battery hybrid system model; in our model, this indicator is controlled via the saturation module. In addition, the voltage value must not drop too quickly, as is reflected in the results shown in Figure 4. Therefore, the results presented in this paper can be considered trustworthy.

With regard to hydrogen production control in SOEC mode, the hybrid system structure used in this paper represents a great improvement on the previous system structure. At the same time, the molar flow rate of hydrogen production and hydrogen consumption need to avoid frequent fluctuation in the hybrid system. This index is highly correlated with the temperature output of the hybrid system, which is fully explained in the literature [12].

It can be seen that the hydrogen consumption/hydrogen production results obtained in this paper meet the requirements of system safety control.

With regard to the control effect of the ADRC controller, the controller proposed in this paper is applicable to the RSOC/Li-ion battery hybrid system. For the output response of the constructed hybrid system mechanism model, the numerical results prove that the ADRC control method has excellent ability to control the complex thermoelectric performance of the hybrid system. We note that there are only two extant papers involving control design for the thermoelectric characteristics of a RSOC/Li-ion battery hybrid system [31,52]. These papers respectively consider RSOC/Li-ion battery hybrid system fuel management and Li-ion battery status management; however, neither considers the control of the heat and power characteristics during the recharging process or attends to rapid adjustments of temperature and voltage. In addition, these works adopt control methods that require precise models, and the proposed control methods all use active disturbance rejection. As these methods do not take into account the automatic adaptation feature of the algorithm, a fair comparison is not possible. The ADRC control proposed in this paper has certain adaptive characteristics when used in a hybrid system.

With regard to the stability of hydrogen production, according to the known mechanism equations (the Nernst voltage model, temperature model, and flow rate model in Table 1), voltage instability can lead to flow rate fluctuations during hydrogen production. In comparing Figures 2b and 6b, we find that under the action of the ADRC controller the hydrogen production in Figure 6b is stable from 40 s to 100 s, leading to the conclusion that the voltage fluctuation effect in Figure 2b is completely suppressed by the ADRC controller.

5. Conclusions

This paper discusses two control problems in an RSOC/Li-ion battery hybrid system during the supply of power to external loads: (i) regulation of the Li-ion battery charging/discharging temperatures and voltage fluctuation; and (ii) control of the thermoelectric performance and hydrogen production in dual-mode (SOFC and SOEC) operation. In the first case, the control problem is aimed at achieving the thermoelectric stability of the Li-ion battery module by reducing voltage fluctuation. In the second case, the purpose of the control problem is to improve power generation/hydrogen production stability in the hybrid system. In this way, it is ensured that the system performs well in terms and stability during power generation/hydrogen production. Moreover, the proposed controller is simple and easy to implement, which makes it suitable for popular implementation in modern industrial production. Another significant advantage is its versatility. This technique can be applied to similar and more complex hybrid system operation processes where a low-order input–output model can be obtained. Although the controller proposed in this paper is based on a validated RSOC/Li-ion battery system model, in order to complete the required experiments it is necessary to consider the effects of relevant operational variables, such as the accumulated battery loss. Future research might focus on applying the ADRC controller proposed in this paper to real versus multiple input–multiple output situations.

Author Contributions: Conceptualization, X.W. and X.L.; methodology, L.H.; software, Y.L. and Z.G.; validation, Y.X., Z.W. and J.P.; formal analysis, Z.X.; writing—original draft preparation, X.W.; writing—review and editing, Y.L.; supervision, X.W. and J.H.; project administration, X.L.; funding acquisition, X.W. and X.L. All authors have read and agreed to the published version of the manuscript.

Funding: This research was funded by the National Natural Science Foundation of China (grant no. 62203204, U2066202, 61873323, 81960327), Jiangxi Provincial Natural Science Foundation (Grant no. 20212BAB212013), Belt and Road Joint Laboratory on Measurement and Control Technology Fund (No. mct202102), the Science, Technology and Innovation Commission of Shenzhen Municipality (Grant no. JCYJ20210324115606017), and National key research and development program (No. 2022YFB4002200).

Institutional Review Board Statement: Not applicable.

Informed Consent Statement: Not applicable.

Data Availability Statement: Not applicable.

Conflicts of Interest: The authors declare no conflict of interest.

References

1. Shi, J.; Zhu, Y.; Feng, Y.; Yang, J.; Xia, C. A Prompt Decarbonization Pathway for Shipping: Green Hydrogen, Ammonia, and Methanol Production and Utilization in Marine Engines. *Atmosphere* **2023**, *14*, 584. [CrossRef]
2. Tang, B.; Xu, Y.; Wang, M. Life cycle assessment of battery electric and internal combustion engine vehicles considering the impact of electricity generation mix: A case study in China. *Atmosphere* **2022**, *13*, 252. [CrossRef]
3. Wu, X.L.; Xu, Y.W.; Li, D.; Zheng, Y.; Li, J.; Sorrentino, M.; Yu, Y.; Wan, X.; Hu, L.; Zou, C.; et al. Afterburner temperature safety assessment for solid oxide fuel cell system based on computational fluid dynamics. *J. Power Sources* **2021**, *496*, 229837. [CrossRef]
4. Yang, D.; Chen, G.; Zhang, L.; Chen, Z.; Zhang, R.; Asghar, M.I.; Geng, S.; Lund, P.D. Low temperature ceramic fuel cells employing lithium compounds: A review. *J. Power Sources* **2021**, *503*, 230070. [CrossRef]
5. Schäfer, F.; Egger, S.; Steiner, D.; Carré, M.; Eichel, A. Control of oxygen-to-carbon ratio and fuel utilization with regard to solid oxide fuel cell systems with anode exhaust gas recirculation: A review. *J. Power Sources* **2022**, *524*, 231077. [CrossRef]
6. Mei, S.; Lu, X.; Zhu, Y.; Wang, S. Thermodynamic assessment of a system configuration strategy for a cogeneration system combining SOFC, thermoelectric generator, and absorption heat pump. *Appl. Energy* **2021**, *302*, 117573. [CrossRef]
7. Tee, J.Z.; Lim, I.L.; Zhou, K.; Anaya-Lara, O. Transient Stability Analysis of Battery with Fuel Cell Driven to Electric Powertrain. In Proceedings of the IECON 2020 the 46th Annual Conference of the IEEE Industrial Electronics Society, Singapore, 18–21 October 2020; pp. 1941–1946.
8. Cen, J.; Li, Z.; Jiang, F. Experimental investigation on using the electric vehicle air conditioning system for lithium-ion battery thermal management. *Energy Sustain. Dev.* **2018**, *45*, 88–95. [CrossRef]
9. Cui, X.; Hu, T. Robust predictive thermal management strategy for lithium-ion battery based on thermoelectric cooler. *Appl. Therm. Eng.* **2023**, *221*, 119833. [CrossRef]
10. Wu, X.; Gao, D. Fault tolerance control of SOFC systems based on nonlinear model predictive control. *Int. J. Hydrogen Energy* **2017**, *42*, 2288–2308. [CrossRef]
11. Li, Y.; Yang, F.; Chen, D.; Hu, S.; Xu, X. Thermal-physical modeling and parameter identification method for dynamic model with unmeasurable state in 10-kW scale proton exchange membrane fuel cell system. *Energy Convers. Manag.* **2022**, *276*, 116580. [CrossRef]
12. Wu, X.L.; Xu, Y.W.; Zhao, D.Q.; Zhong, X.; Li, D.; Jiang, J.; Deng, Z.; Fu, X.; Li, X. Extended-range electric vehicle-oriented thermoelectric surge control of a solid oxide fuel cell system. *Appl. Energy* **2020**, *263*, 114628. [CrossRef]
13. Qin, X.; Cao, J.; Geng, G.; Li, Y.; Zheng, Y.; Zhang, W.; Yu, B. Solid oxide fuel cell system for automobiles. *Int. J. Green Energy* **2022**. [CrossRef]
14. Han, Y.; Li, J.; Wang, B. Event-Triggered Active Disturbance Rejection Control for Hybrid Energy Storage System in Electric Vehicle. IEEE *Trans. Transp. Electrif.* **2022**, *9*, 75–86. [CrossRef]
15. Long, B.; Zeng, W.; Rodríguez, J.; Garcia, C.; Guerrero, J.; Chong, K. Stability Enhancement of Battery-Testing DC Microgrid: An ADRC-Based Virtual Inertia Control Approach. *IEEE Trans. Smart Grid* **2022**, *13*, 4256–4268. [CrossRef]
16. Chen, X.; Xu, J.; Liu, Q.; Chen, Y.; Wang, X.; Li, W.; Ding, Y.; Wan, Z. Active disturbance rejection control strategy applied to cathode humidity control in PEMFC system. *Energy Convers. Manag.* **2020**, *224*, 113389. [CrossRef]
17. Wang, P.; Ma, Y.; Li, J.; Gao, Y.; Zhang, Y.; Ma, D. A Novel Control Algorithm of the Air Supply Subsystem: Based on Dynamic Modeling of Proton Exchange Membrane Fuel Cell. *Processes* **2022**, *10*, 1499. [CrossRef]
18. Zhong, S.; Huang, Y.; Guo, L. A parameter formula connecting PID and ADRC. *Sci. China Inf. Sci.* **2020**, *63*, 1–13. [CrossRef]
19. Zhong, S.; Huang, Y.; Guo, L. An ADRC-based PID tuning rule. *Int. J. Robust Nonlinear Control.* **2022**, *32*, 9542–9555. [CrossRef]
20. Xue, W.; Huang, Y. Comparison of the DOB based control, a special kind of PID control and ADRCC. In Proceedings of the 2011 American Control Conference, San Francisco, CA, USA, 29 June–1 July 2011; pp. 4373–4379. [CrossRef]
21. Wu, G.; Sun, L.; Lee, K.Y. Disturbance rejection control of a fuel cell power plant in a grid-connected system. *Control. Eng. Pract.* **2017**, *60*, 183–192.
22. Curiel-Olivares, G.; Linares-Flores, J.; Guerrero-Castellanos, J.F.; Hernández-Méndez, A. Self-balancing based on active disturbance rejection controller for the two-in-wheeled electric vehicle, experimental results. *Mechatronics* **2021**, *76*, 102552. [CrossRef]
23. Hezzi, A.; Ben Elghali, S.; Bensalem, Y.; Zhou, Z.; Benbouzid, M.; Abdelkrim, M. ADRC-based robust and resilient control of a 5-phase PMSM driven electric vehicle. *Machines* **2020**, *8*, 17. [CrossRef]
24. Liu, C.; Luo, G.; Zhe, C.; Wencong, T.; Cai, Q. A linear ADRC-based robust high-dynamic double-loop servo system for aircraft electro-mechanical actuators. *Chin. J. Aeronaut.* **2019**, *32*, 2174–2187. [CrossRef]
25. Guo, B.; Bacha, S.; Alamir, M. A review on ADRC based PMSM control designs. In Proceedings of the IECON 2017—43rd Annual Conference of the IEEE Industrial Electronics Society, Beijing, China, 29 October–1 November 2017; pp. 1747–1753. [CrossRef]
26. Sahoo, S.; Amirthalakshmi, T.M.; Ramesh, S.; Ramkumar, G.; Arockia Dhanraj, J.; Ranjith, A.; Obaid, S.; Alfarraj, S.; Kumar, S. Artificial Deep Neural Network in Hybrid PV System for Controlling the Power Management. *Int. J. Photoenergy* **2022**, *2022*, 9353470.

27. Heidary, J.; Gheisarnejad, M.; Khooban, M.H. Stability Enhancement and Energy Management of AC-DC Microgrid based on Active Disturbance Rejection Control. *Electr. Power Syst. Res.* **2023**, *217*, 109105. [CrossRef]
28. Kamran, H.; Mudassir, U.; Ali, A.M.; Kamal, K.; Ratlamwala, T.A.H.; Raza, M.A.; Khan, K. Simulation and modeling of copper-chlorine cycle, molten carbonate fuel cell alongside a heat recovery system named regenerative steam cycle and electric heater with the incorporation of PID controller in MATLAB/SIMULINK. *Int. J. Hydrogen Energy* **2022**, *47*, 40462–40475. [CrossRef]
29. Erixno, O.; Abd Rahim, N.; Ramadhani, F.; Adzman, N.N. Energy management of renewable energy-based combined heat and power systems: A review. *Sustain. Energy Technol. Assessments* **2022**, *51*, 101944. [CrossRef]
30. Xia, Z.; Deng, Z.; Jiang, C.; Zhao, D.; Kupecki, J.; Wu, X.; Xu, Y.; Liu, G.; Fu, X.; Li, X. Modeling and analysis of cross-flow solid oxide electrolysis cell with oxygen electrode/electrolyte interface oxygen pressure characteristics for hydrogen production. *J. Power Sources* **2022**, *529*, 231248. [CrossRef]
31. Xu, Y.; Wu, X.; Zhong, X.; Zhao, D.; Fu, J.; Jiang, J.; Deng, Z.; Fu, X.; Li, X. Development of solid oxide fuel cell and battery hybrid power generation system. *Int. J. Hydrogen Energy* **2020**, *45*, 8899–8914. [CrossRef]
32. Zhang, L.; Jiang, J.; Cheng, H.; Deng, Z.; Li, X. Control strategy for power management, efficiency-optimization and operating-safety of a 5-kW solid oxide fuel cell system. *Electrochim. Acta* **2015**, *177*, 237–249. [CrossRef]
33. Cheng, H.; Jing, S.; Xu, Y.; Deng, Z.; Li, J.; Li, X. Control-oriented modeling analysis and optimization of planar solid oxide fuel cell system. *Int. J. Hydrogen Energy* **2016**, *41*, 22285–22304. [CrossRef]
34. Tansini, A.; Fontaras, G.; Millo, F. A Multipurpose Simulation Approach for Hybrid Electric Vehicles to Support the European CO_2 Emissions Framework. *Atmosphere* **2023**, *14*, 587. [CrossRef]
35. Sun, W.; Huo, J.; Fu, Q.; Zhang, Y.; Lin, X. Influence of meteorological factors and chemical processes on the explosive growth of PM2. 5 in Shanghai, China. *Atmosphere* **2022**, *13*, 1068. [CrossRef]
36. Nassef, A.M.; Rezk, H.; Alahmer, A.; Abdelkareem, M.A. Maximization of CO_2 Capture Capacity Using Recent RUNge Kutta Optimizer and Fuzzy Model. *Atmosphere* **2023**, *14*, 295. [CrossRef]
37. He, Y.; Chen, G.; Zhang, X.; Zhang, L.; Yang, D.; Asghar, M.I.; Geng, S.; Lund, P.D. Mechanism for major improvement in SOFC electrolyte conductivity when using lithium compounds as anode. *Acs Appl. Energy Mater.* **2020**, *3*, 4134–4138. [CrossRef]
38. Zhang, X.; Wei, Q.S.; Oh, B.S. Cost analysis of off-grid renewable hybrid power generation system on Ui Island, South Korea. *Int. J. Hydrogen Energy* **2022**, *47*, 13199–13212. [CrossRef]
39. Zhang, Z.; Zhou, J.; Zong, Z.; Chen, Q.; Zhang, P.; Wu, K. Development and modelling of a novel electricity-hydrogen energy system based on reversible solid oxide cells and power to gas technology. *Int. J. Hydrogen Energy* **2019**, *44*, 28305–28315. [CrossRef]
40. Cao, H.; Li, X.; Deng, Z.; Jiang, J.; Yang, J.; Li, J.; Qin, Y. Dynamic modeling and experimental validation for the electrical coupling in a 5-cell solid oxide fuel cell stack in the perspective of thermal coupling. *Int. J. Hydrogen Energy* **2011**, *36*, 4409–4418. [CrossRef]
41. Gao, L.; Liu, S.; Dougal, R.A. Dynamic lithium-ion battery model for system simulation. *IEEE Trans. Components Packag. Technol.* **2002**, *25*, 495–505.
42. Rahn, C.D.; Wang, C.Y. *Battery Systems Engineering*; John Wiley & Sons: Hoboken, NJ, USA, 2013. [CrossRef]
43. Liu, S.; Zhang, Y.L.; Xue, W.; Shi, G.; Zhu, M.; Li, D. Frequency response-based decoupling tuning for feedforward compensation ADRC of distributed parameter systems. *Control. Eng. Pract.* **2022**, *126*, 105265.
44. Zhan, B.; Zhang, L.; Liu, Y.; Gao, J. Model predictive and compensated ADRC for permanent magnet synchronous linear motors. *Isa Trans.* 2022, *in Press*. [CrossRef]
45. Chen, W.; Wang, S.; Li, J.; Lin, C.; Yang, Y.; Ren, A.; Li, W.; Zhao, X.; Zhang, W.; Guo, W.; et al. An ADRC-based triple-loop control strategy of ship-mounted Stewart platform for six-DOF wave compensation. *Mech. Mach. Theory* **2023**, *184*, 105289. [CrossRef]
46. Han, J. From PID to active disturbance rejection control. *IEEE Trans. Ind. Electron.* **2009**, *56*, 900–906. [CrossRef]
47. Tan, W.; Chang, S.; Zhou, R. Load frequency control of power systems with non-linearities. *IET Gener. Transm. Distrib.* **2017**, *11*, 4307–4313. [CrossRef]
48. Li, D.; Li, C.; Gao, Z.; Jin, Q. On active disturbance rejection in temperature regulation of the proton exchange membrane fuel cells. *J. Power Sources* **2015**, *283*, 452–463. [CrossRef]
49. Li, G.; Fu, H.; Madonski, R.; Czeczot, J.; Nowak, P.; Lakomy, K.; Sun, L. Feed-forward offset-free model predictive temperature control for proton exchange membrane fuel cell: An experimental study. *Isa Trans.* **2022**, *128*, 159–170. [CrossRef]
50. Chen, S.C.; Wan, C.C.; Wang, Y.Y. Thermal analysis of lithium-ion batteries. *J. Power Sources* **2005**, *140*, 111–124. [CrossRef]
51. Xue, T.; Wu, X.; Zhao, D.; Xu, Y.; Jiang, J.; Deng, Z.; Fu, X.; Li, X. Fault-tolerant control for steam fluctuation in SOFC system with reforming units. *Int. J. Hydrogen Energy* **2019**, *44*, 23360–23376. [CrossRef]
52. Ran, P.; Zhou, X.; Wang, Y.; Fan, Q.; Xin, D.; Li, Z. Thermodynamic and exergetic analysis of a novel multi-generation system based on SOFC, micro-gas turbine, s-CO_2 and lithium bromide absorption refrigerator. *Appl. Therm. Eng.* **2023**, *219*, 119585. [CrossRef]